Kobe J. Med. Sci., Vol. 48, No. 3, pp. 87-96, 2002

A Voltage-gated H^+ Channel is a Powerful Mechanism for pH Homeostasis in Murine Osteoclasts

HIROYUKI MORI, HIROMU SAKAI, HIROKAZU MORIHATA, TSUNEKAZU YAMANO*, and MIYUKI KUNO

Departments of Physiology and Pediatrics, Osaka City University Graduate School of Medicine, Abeno-ku, Osaka 545-8585, Japan*

Received 1 October 2002/ Accepted 11 November 2002

Key words: proton channel; pH regulation; osteoclast; osteoclastogenesis; bone resorption

Osteoclasts secrete a large amount of proton (H^+) ions and proteolytic enzymes into bone resorption pit to degrade bone matrix. In addition to H^+ pumps and exchangers, voltage-gated H^+ channels, which are H^+ conductive pathways, are expressed in osteoclasts. H^+ channels are distinct in their strong H^+ extrusion ability, but the functional role is not clear. This is the first study of H^+ channels in murine osteoclasts generated from mononuclear precursors in the presence of a soluble form of receptor activator of nuclear factor kappa B ligand (RANKL) and macrophage colony stimulating factor (M-CSF). The H^+ channel was characterized by voltage- and pH-dependent activation, slow activation kinetics, and outward rectification. The reversal potential (V_{rev}) was shifted to more positive potentials by decreasing the pH gradient across the plasma membrane (ΔpH). Employing V_{rev} as a real time monitor of pH in clamped cells, it is revealed that the H^+ channel activation could decrease ΔpH by ~0.43 unit/s. Decline in the current during prolonged depolarizations was accompanied by a positive shift in V_{rev}. This implies that the H^+ channel activity is auto-regulated by sensing ΔpH, to compensate for pH imbalance. The H^+ current-density in cells with $\geq$6 nuclei was significantly smaller than that in cells with $\leq$5 nuclei, although the activation rate was unaltered. Thus, the H^+ channel activity may alter during osteoclastogenesis. These data suggest the H^+ channel is a powerful mechanism for pH homeostasis of osteoclasts that are exposed to drastic change in pH environments during the bone resorption cycle.

Osteoclasts adhere to bone surface and degrade bone matrix by secreting proton ions (H^+) and proteolytic enzymes into a sealed compartment formed between osteoclast and bone surface. During the bone-remodeling process, osteoclasts are exposed to drastic changes in the pH of the intracellular and extracellular microenvironments. Diverse mechanisms, such as, vacuolar type H^+-ATPases (V-ATPases), Na^+/H^+ exchangers and Cl^-/HCO_3^- exchangers are involved in H^+-secretion and regulation of intracellular pH (pH_i) in osteoclasts (24). In addition to the pumps and ion exchangers, a voltage-gated H^+ channel was found in rabbit osteoclasts (22). Voltage-gated H^+ channels possess strong H^+-extruding ability and have been considered to be a potent regulator of pH_i and the membrane potential in many types of cells (4). The H^+ current activity is high in phagocytic cells, like neutrophils (2), macrophages (11) and microglia (6,19). As osteoclasts are originated from granulocyte-macrophage lineage of hematopoietic stem cells in bone marrow (GM-CFU), it is no wonder that H^+ channels may play specific roles in regulating osteoclast function. However, literature on H^+ channels in osteoclasts is scarce, and their functional role remains

Phone: 81-6-6645-3711 Fax: 81-6-6645-3712 E-mail: morih@med.osaka-cu.ac.jp

unclear.

The purpose of the present study was to investigate properties and activities of the H^+ channel in murine osteoclasts during osteoclastogenesis. The difficulty in using freshly isolated osteoclasts is associated with the paucity and cell damages caused by the isolation procedures. In addition, osteoclastogenesis are influenced by various factors, some of which might differ from preparation to preparation. To overcome these problems, we used an *in vitro* culture system in which mononuclear osteoclast precursors fuse with each other into multinuclear osteoclasts in the presence of a soluble form of receptor activator of nuclear factor kappa B ligand (RANKL) and macrophage colony stimulating factor (M-CSF) (21,31). We found that murine osteoclasts expressed a H^+ channel that shared the electrophysiological features with "type *p*" H^+ channels in phagocytes. The H^+ channel could contribute to rapid compensation for pH imbalance across the plasma membrane, and the activity may alter during the bone resorption cycle and osteoclastogenesis. A preliminary account has been made (17).

MATERIALS AND METHODS

Cells. Osteoclasts were generated from bone marrow cells of male, 5 to 8-week-old C3H/HeN mice as described elsewhere (21, 31). Bone marrow cells were obtained from the tibias and femurs, centrifuged at 700 *g* for 7 min at 4°C, and suspended in 1 ml of α-minimum essential medium (α-MEM) supplemented with 15% fetal calf serum (FCS), 0.1 mg/ml streptomycin and 100 U/ml penicillin. The cell suspension was then placed on a chromatography column filled with 5 ml of Sephadex G10 gel (Amersham Pharm Biotech) and was incubated at 37°C in a 95% air-5% CO_2 atmosphere for 45 min. After removing adherent cells by means of gel filtration, non-adherent cells were centrifuged at 700 *g* for 7 min at 4°C and plated on glass coverslips at 2 x 10^7 cells/ml in a fresh medium containing 10 - 20 ng/ml of macrophage colony stimulating factor (M-CSF) (Peprotec) and 50 - 100 ng/ml of a soluble form of receptor activator of nuclear factor kappa B ligand (RANKL) (Peprotec). Coverslips were coated with M-CSF (10 – 20 ng/ml). Half of the medium was changed every two - three days. Multinuclear cells appeared within 5 days in culture and were maintained for 10-15 days. Osteoclasts were identified with the phase-contrast microscopy as multinucleated cells with tartrate-resistant acid phosphatase (TRAP) activity (28,29).

Electrophysiological recordings. Whole cell currents were obtained as described elsewhere (28, 29). Briefly, current signals were recorded with an amplifier (Axopatch 200A, Axon Instruments), digitized at 2 kHz with an analog-digital converter and analyzed using pCLAMP software at room temperature (20-24°C). The borosilicate glass pipettes had a resistance of 5-8 MΩ. The series resistance compensation (60-80%) was conducted to reduce the voltage error. The reference electrode was a Ag-AgCl wire connected to the bath solution through a Ringer-agar bridge. The zero current potential before formation of the gigaseal was taken as 0 mV. Data were expressed as means ± S.E.M., and tested using Student's unpaired *t*-test.

The external solution contained (mM): 75 N-methyl D-glucamine (NMDG)-aspartate, 1 $CaCl_2$, 1 $MgCl_2$, 10 glucose, 0.1% BSA, 80-100 Hepes (pH = 6.8 – 7.8). To block Cl^- channels, 100 μM of 4,4'-diisothiocyanato-2, 2'-stilbenesulfonate (DIDS) was added to the bath (28,29). The pipette solutions contained (mM): 65 NMDG-aspartate or 75 Cs-methanesulfonate, 3 $MgCl_2$, 1 BAPTA or 1 EGTA, 5 Na_2ATP, 120 Mes or 100 Hepes (pH = 5.5 – 7.8). The pH buffers, Mes and Hepes, were used to make the pipette solutions of $pH_p<7.0$ and ≥ 7.0, respectively. The calcium buffer, BAPTA, was substituted by EGTA when the pH of the solutions was ≤6.8. The pH of the bath and pipette solutions (pH_o and pH_p) was

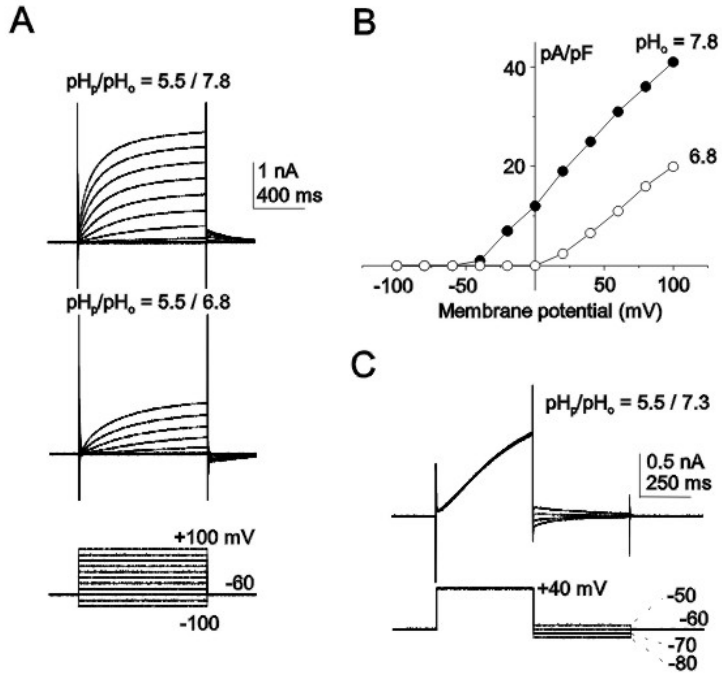

FIG. 1. pH-dependence of whole cell currents in murine osteoclasts. (A) a family of currents evoked by voltage steps (1 s) in 20 mV increments applied at –60 mV. The pH_p/pH_o was 5.5/7.8 (upper) and 5.5/6.8 (lower). (B) current-voltage (I-V) relationships for the current amplitudes measured at the end of 1 s-long voltage steps in A. Decreasing pH_o shifted the I-V curve to more positive potentials. (C) instantaneous tail currents at -80 - -50 mV following a depolarization prepulse (+40 mV, 500 ms). pH_p/pH_o = 5.5/7.3. Cells were bathed in the external solution containing NMDG-aspartate and 100 μM DIDS. The pipette solution contained Cs-methanesulfonate.

adjusted by CsOH. The osmolality of the solutions was maintained between 280-300 mosmol/l.

Chemicals. Mes and BAPTA were purchased from Dojindo Laboratories. All other chemicals were obtained from Sigma Chemical Co. A condensed stock solution of Na_2ATP (500 mM) was prepared in 1 M Tris Cl, stored in a freezer, and added to the internal medium before use. A stock solution of DIDS was dissolved in dimethyl sulphoxide (DMSO). The final concentration of DMSO (≤0.1%) did not affect the membrane currents.

RESULTS

Voltage-gated H^+ currents of murine osteoclasts.

Murine osteoclasts have been reported to possess K^+ and Cl^- channels (25,26,27,28,29). To block these channels, major ions (Na^+, K^+, Cl^-) were replaced by the impermeable substitutes ($NMDG^+$, Cs^+, $aspartate^-$) and a Cl^- channel blocker, DIDS (100 μM), was added to the external solution. Figure 1A shows representative whole cell currents in osteoclasts generated in the presence of sRANKL and M-CSF under a large pH gradient across the plasma membrane (ΔpH) (pH_p/pH_o = 5.5/7.8 and 5.5/6.8). Slowly-activated outward currents

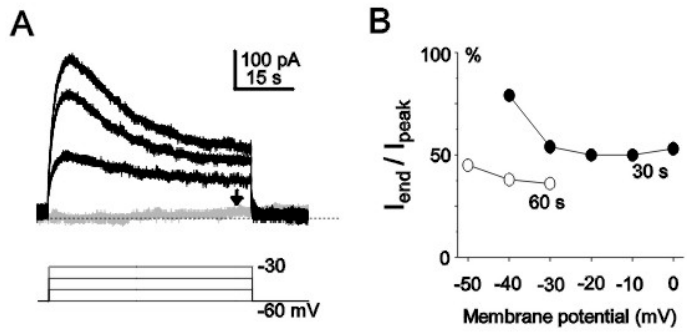

FIG. 2. Decline of H^+ currents during long-lasting depolarization. (A) H^+ currents evoked by 60 s-long depolarizations from -50 to -30 mV. Small outward currents were activated slowly even at -60 mV (gray trace with an arrow). At more positive potentials, the current decreased after the peak. (B) current amplitudes at the end of long depolarizations were expressed as percent of its peak amplitude and plotted against the membrane potential. Data were obtained from two cells stimulated by either 30 s- or 60 s- long depolarizations. pH_p/pH_o = 5.5/7.3.

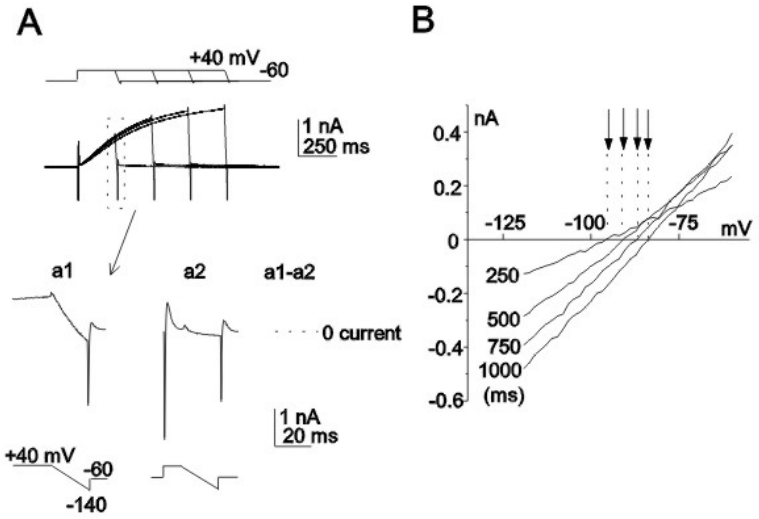

FIG. 3. Shift of the reversal potential accompanying activation of H^+ currents. (A) H^+ currents recorded with a ramp-repolarization method. A 20 ms-long repolarizing voltage ramp from +40 to -140 mV was applied following 250, 500, 750 and 1000 ms-long prepotentials (+40 mV). In **a1**, the current trace with a 250 ms-long prepotential is magnified. As the H^+ current has slow activation kinetics, leak and capacitative currents were obtained with a short prepotential (+40 mV, 10 ms) (**a2**). Subtraction (**a1 – a2**) yields the net H^+ current flowing during the voltage-ramp. (B) I-V relationships for the net H^+ currents along the repolarization ramp pulse. The reversal potential (V_{rev}, arrows) shifted from -96 mV (250 ms) to -83 mV (1000 ms). pH_p/pH_o = 5.5/7.3.

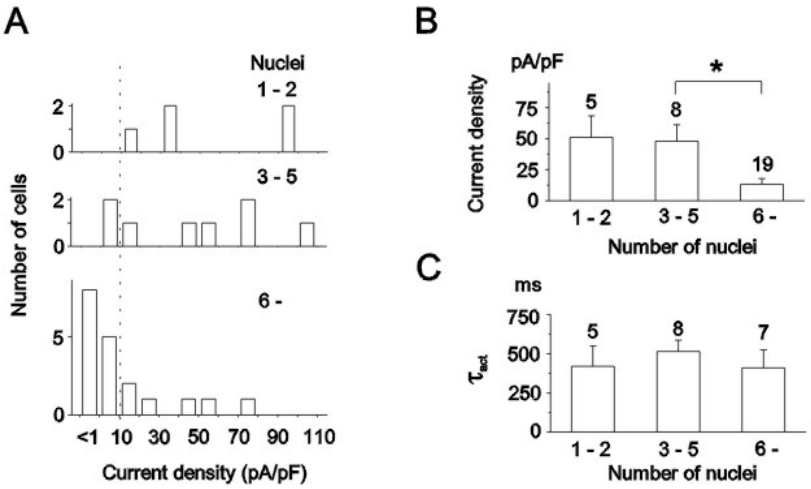

FIG. 4. H^+ currents during different stages of osteoclastogenesis. (A) distributions of the H^+ current-density in cells with ≤ 2 nuclei (top), 3-5 nuclei (middle) and ≥ 6 nuclei (bottom). Bin size: 10 pA/pF, except for data ≤ 10 pA/pF. Data ≤ 10 pA/pF were divided into two groups, <1 and ≥1 pA/pF. (B and C) averaged current-density (B) and activation time constant (τ_{act}) (C) in cells with ≤ 2, 3-5 and ≥ 6 nuclei. Data (means ± S. E. M.) were obtained by 1 s-long depolarization (+100 mV) applied at –60 mV. pH_p/pH_o = 5.5/7.3. * p <0.01.

were evoked by depolarizing voltage steps applied at a holding potential of -60 mV. Decreasing pH_o reduced the current amplitude and activation rate at any given voltage (FIG. 1A, lower), and shifted the current-voltage (I-V) relationship to more positive potentials (FIG. 1B). The reversal potential (V_{rev}) estimated from instantaneous tail currents at different potentials (FIG. 1C) was –58 ± 6 mV (n = 4) at ΔpH of 1.8. Decreasing ΔpH by 0.5 unit shifted V_{rev} to more positive potentials by 21 ± 8 mV (4) without changes in concentrations of other ions, suggesting that H^+ was a major charge carrier for the outward current.

Quick compensation of pH imbalance by H^+ channels.

As the activation rate was slow at low voltages (FIG. 1A), outward H^+ currents were often recognized only at large depolarizations when the short (1 s-long) voltage-pulse protocol was used (FIG. 1). When long-lasting (60 s) depolarizations were applied, the H^+ current was detected at the lower potentials, < -30 mV under pH_p/pH_o 5.5/7.3 (FIG. 2A). Even at the holding potential, -60 mV, the H^+ channel was activated, although it was very slowly (the bottom trace with an arrow).

The long-pulse protocol also revealed that the current amplitude declined after a peak during the depolarization (FIG. 2A). Figure 2B shows the ratio between the current amplitude at the end of depolarization (I_{end}) and that at its peak (I_{peak}) in two cells stimulated with 30 s- and 60 s-long voltage-steps: the inhibition was enhanced by prolongation of the depolarization. The I_{end}/I_{peak} was smaller at more depolarized voltages, but maintained to be constant at ≥ -30 mV. Although this relaxation of the H^+ current was not evident within the short (≤1 s) voltage-pulse protocol (FIG. 1A, C), amplitudes of the H^+ current decreased

gradually when the depolarization was repeated at short intervals (FIG. 3A, top). Therefore, neither voltage nor duration of depolarization was primary to this phenomenon.

It has been thought that H^+ channels do not inactivate during depolarization (4). The rundown may be due to decreases in the electromotive force for H^+ by preceding H^+ efflux through the H^+ channel. To confirm this hypothesis, V_{rev} following depolarizations of different durations was measured using a ramp repolarization method (7): 20 ms-long repolarization voltage-ramps were applied following sequential depolarizations (+40 mV) of 250, 500, 750 and 1000 ms (FIG. 3A, top). Subtraction of the capacitative and leak currents yielded the net H^+ current passing through the open channel (a1 - a2). V_{rev}, determined by zero-current potential from I-V curves for the net current, was shifted to more positive potentials by extending the depolarization period (FIG. 3B arrows). The amount of the shift of V_{rev} within 1 s varied greatly among cells: 12 ± 3 mV (n = 7; 4 ~ 25 mV). This positive shift in V_{rev} corresponded to a decrease in ΔpH of 0.21 ± 0.05 unit (n = 7; 0.07 – 0.43). Therefore, the H^+ channel could compensate for pH imbalance across the plasma membrane very rapidly. The resultant decrease in ΔpH would lead to the decline of the H^+ current. The H^+ channel activity seems to be regulated exquisitely in response to changes in ΔpH.

H^+ channel activity during osteoclastogenesis.

Each culture dish contained cells with nuclei from one to >20. Figure 4A shows distributions of the current-density under pH_p/pH_o 5.5/7.3 (100 mV, 1 s) in cells cultivated for 5-6 days in vitro: cells were classified into three groups with ≤2, 3-5 and ≥6 nuclei. The H^+ current varied greatly among cells: there was no apparent change between the former two groups, but, in 8 of 19 cells (45%) with ≥6 nuclei, the H^+ current was negligible or only slight (leftmost column; < 1 pA/pF). The averaged H^+ current density (+100 mV, 1 s) was 51 ± 13 pA/pF (n = 5) in cells with ≤2 nuclei, 48 ± 13 pA/pF (n = 8) with 3-5 nuclei, and was significantly smaller than the other two groups in cells with ≥6 nuclei, 13 ± 5 pA/pF (n = 19) ($p < 0.01$) (FIG. 4B). The high H^+ current-density in cells with ≤2 nuclei was confirmed under different experimental conditions: ≥25 pA/pF at lower ΔpH (pH_p/pH_o 6.0/7.3) or at more negative voltages (+20 mV) (n = 3). The cell capacitance in cells with ≤2, 3-5 and ≥6 nuclei was 44 ± 5 pF (n = 8), 50 ± 6 pF (n = 8) and 140 ± 25 pF (n = 19), respectively, indicating that on the average, cell size increased accompanying osteoclastogenesis. However, an increase in the cell area was unlikely to be the determinant for the low current-density: although a subpopulation of osteoclasts with ≥6 nuclei had cell capacitance similar to cells with ≤5 nuclei, the current-density was significantly smaller than that in cells with 3-5 nuclei (20 ± 11 pA/pF, 57 ± 8 pF, n = 7) ($p < 0.05$).

The activation time constant (τ_{act}), estimated from the single exponential fit for the activation time course at 100 mV, did not alter among the three groups: 420 ± 130 ms at 100 mV (n =5) with 1-2 nuclei, 520 ± 70 ms (n = 8) with 3-5 nuclei and 410 ± 120 ms (n = 8) with ≥6 nuclei (FIG. 4B). Therefore, the gating property of the H^+ channel was preserved during maturation of osteoclasts, suggesting that either the number of available channels or the single channel conductance may decrease during osteoclastogenesis.

DISCUSSION

The present study provides the first description of the voltage-gated H^+ channel in murine osteoclasts. The electrophysiological features, such as, voltage-dependent activation, slow activation kinetics, pH-dependency and outward rectification, are common with those reported in rabbit osteoclasts (22) and in other types of macrophage lineage (4). Based on classification of H^+ channels by gating properties, the H^+ channel in murine osteoclasts resembles type *p* channels expressed in phagocytes (1).

Potent pH regulating ability of H^+ channels. H^+ channels are considered to be $>10^6$ -10^8 times more permeable to H^+ than to other ions (4). The H^+ channel in murine osteoclasts preserved this high selectivity for H^+. That is, the V_{rev} was shifted only by changing ΔpH, while the concentration of H^+ was as low as <1 μM. In addition, the V_{rev} values were far from those for other ions (Na^+, K^+, Cl^- and Ca^{2+}). The V_{rev} of the H^+ current, however, deviated somewhat from the equilibrium potential for H^+ (E_H) predicted by the Nernst equation, partly due to imperfect control of pH_i with the buffer action of the pipette solutions (4). In addition, the inherent nature of the H^+ channels may affect the measurement: ΔpH decreases by H^+ efflux during the voltage-pulse protocols used to determine V_{rev}. In general, the deviation of V_{rev} from E_H was larger with the instantaneous tail method than the ramp repolarization method, probably because repeated depolarizations in the former method would result in more H^+ efflux.

The V_{rev} of the H^+ channel could work as a real time monitor of pH changes in clamped cells. The ramp repolarization method has revealed that the H^+ channel could change pH greatly even within a short period < 1 s. The decrease in ΔpH during 1 s-long depolarization of +40 mV, estimated from the shift of V_{rev}, was 0.07 ~ 0.43 unit at room temperature. This remarkable pH regulating ability of the H^+ channel may be enhanced at physiological temperature, as H^+ channels are highly sensitive to temperature (3,14). Decreases in ΔpH would lead to a reduction of the current amplitude, slow the activation rate and shift the activation threshold to more positive potentials. Decline of the current during prolonged or repetitive depolarizations was caused by the decrease in ΔpH. Neither voltage nor time seemed to be primary to the decline in the H^+ current: it was observed even at low potentials near the holding potential (-60 mV) and after repetition of short (1 s) depolarizations, as reported in microglia (18). The H^+ channel activity seems to be under feedback control by its intrinsic nature, that is, ΔpH dependency of the channel activity.

When is the H^+ channel activated? Threshold potential for activation of H^+ channels is considered to be as follows: $V_{threshold} = 20\ mV - 40\ mV \times \Delta pH$ (4). In general, H^+ channels are apt to open when cells were intracellularly acidified and/or depolarized. Intracellular acidification is induced when osteoclasts are exposed to high concentrations of extracellular Ca^{2+} during bone resorption (8). High extrtracelluar Ca^{2+} inhibits the inwardly rectifying K^+ channel, a major resting conductance of osteoclasts, which causes depolarization (29). In phagocytes, H^+ channels are activated during respiratory bursts due to the excess H^+ liberated at the intracellular surface in association with electron transfer from inside to outside of cells via NADPH oxidases (9). Osteoclasts that originate from granulocyte-macrophage lineage (GM-CFU) express the NADPH oxidase complex at the ruffled membrane (30). H^+ channels in osteoclasts would be activated with the actions of the oxidases, as generation of superoxide has been reported to be involved in bone resorption (13,32). Thus, osteoclasts may encounter favorable conditions to activate the H^+ channel during the resorption cycle.

In addition, the channel activity is controlled by diverse mechanisms both directly and indirectly. For examples, $V_{threshold}$ shifts to more negative potentials by cell swellings and phorbol esters (5), and the H^+ channel activity is enhanced by protein kinase C (5,12,20), arachidonates (2,10) and cell swellings (19). Interactions between these factors may diversify the channel regulation: cell acidosis induces cell swellings (27), which potentiates the H^+ channels (19), although the current-density decreases after chronic acidosis in rabbit osteoclasts (23).

Osteoclasts produce a large amount of H^+ by catalyzing H_2O and CO_2 with carbonic anhydrase type II (CA II). This specialized H^+ metabolism may affect the pH environment, but it is little known about the functional roles of H^+ channels in osteoclasts. In the present *in*

vitro culture system, the H^+ current-density was high in cells with 1-5 nuclei, but was only slight in ~45% of cells with ≥6 nuclei. In rabbit osteoclasts, the pH_i regulatory mechanisms differ between small and large cells (15). Considering that many intracellular and extracellular factors modulate pH_i regulatory mechanisms (16,24), the contribution of the H^+ channel to osteoclast functions may vary with their cellular conditions (22). We hypothesize that the H^+ channels can operate as a potent regulator of pH homeostasis of osteoclasts when they are exposed to drastic changes in the pH environments during the bone resorption cycle.

ACKNOWLEDGEMENT

We thank Drs. S. Matsuura, Y. Watanabe, and F. Nakamura for encouragement through this study, Dr. H. Amano for helpful advice on the culture of osteoclasts, Ms. J. Kawawaki for technical assistance, Ms. C. H. Kim for preparation of this manuscript and Ms. T. Akiyama for secretarial assistance. This work was supported by grants from The Assistant Program of Graduate Student Fellowships of Osaka City University, The Hoansha Foundation, and The Grant-in-Aid for Scientific Research from The Ministry of Education, Science and Culture, Japan.

REFERRENCES

1. **DeCoursey, T. E.** 1998. Four varieties of voltage-gated proton channels. Frontiers Biosci **3**:477-482.
2. **DeCoursey, T. E. and V. V. Cherny.** 1993. Potential, pH, and arachidonate gate hydrogen ion currents in human neutrophils. Biophys. J. **65**:1590-1598.
3. **DeCoursey, T. E. and V. V. Cherny.** 1998. Temperature dependence of voltage-gated H^+ currents in human neutrophils, rat alveolar epithelial cells, and mammalian phagocytes. J. Gen. Physiol. **112**:503-522.
4. **DeCoursey, T. E. and V. V. Cherny.** 2000. Common themes and problems of bioenergetics and voltage-gated proton channels. 2000. Biochim Biophys Acta **1458**:104-119.
5. **DeCoursey, T. E., V. V. Cherny, A. G. DeCoursey, W. Xu, and L. L. Thomas.** 2001. Interactions between NADPH oxidase-related proton and electron currents in human eosinophils. J. Physiol. **535**:767-781.
6. **Eder, C., H. G. Fischer, U. Hadding, and U. Heinemann.** 1995. Properties of voltage-gated currents of microglia developed using macrophage colony-stimulating factor. Pfügers Arch. **430**:526-533.
7. **Gordienko, D. V., M. Tare, S. Parveen, C. J. Fenech, C. Robinson, and T. B. Bolton.** 1996. Voltage-activated proton current in eosinophils from human blood. J. Physiol. **496**:299-316.
8. **Grano, M., R. Faccio, S. Colucc, R. Paniccia, N. Baldini, A. Z. Zallone, and A. Teti.** 1994. Extracellular Ca^{2+} sensing is modulated by pH in human osteoclast-like cells in vitro. Am. J. Physiol. **267**:C961-968.
9. **Henderson, L. M. and J. B. Chappell.** 1992. The NADPH-oxidase-associated H^+ channel is opened by arachidonate. Biochem. J. **283**:171-175.
10. **Henderson, L. M., G. Banting, and J. B. Chappell.** 1995. The arachidonate-activable, NADPH oxidase-associated H^+ channel. J. Biol. Chem. **270**:5909-5916.
11. **Kapus, A., R. Romanek, A. Y. Qu, O. D. Rotstein, and S. Grinstein.** 1993. A pH-sensitive and voltage-dependent proton conductance in the plasma membrane of macrophages. J. Gen. Physiol. **102**: 729-760.
12. **Kapus, A., K. Szaszi, and E. Ligeti.** (1992). Phorbol 12-myristate 13-acetate activates an electrogenic H^+-conducting pathway in the membrane of neutrophils. Biochem. J. **281**:697-701.
13. **Key, L. L. Jr., W. C. Wolf, C. M. Gundberg, and W. L. Ries.** 1994. Superoxide and bone resorption. Bone. **15**:431-436.
14. **Kuno, M., J. Kawawaki, and F. Nakamura.** 1997. A highly temperature-sensitive proton current in mouse bone marrow-derived mast cells. J. Gen. Physiol. **109**:731-740.
15. **Lees, R. L. and J. N. Heersche.** 2000. Differences in regulation of pH_i in large (≥10 nuclei) and small (≥10 nuclei) osteoclasts. Am. J. Physiol. **279**:C751-761.
16. **Lehenkari, P. P., T. Laitala-Leinonen, T. –J. Linna, and H. K. Väänänen.** 1997. The regulation of pH_i in osteoclasts is dependent on the culture substrate and on the stage of the resorption cycle. Biochem. Biophys. Res. Commun. **235**:838-844.
17. **Mori, H., H. Sakai, H. Morihata, K. Sakuta, and M. Kuno.** 2001. A voltage-gated proton channel in murine osteoclasts during development from bone marrow cells. J. Bone Miner. Res. **16 (Supple)**:S377.
18. **Morihata, H., J. Kawawaki, H. Sakai, M. Sawada, T. Tsutada, and M. Kuno.** 2000. Temporal fluctuation of voltage-gated proton currents in rat spinal microglia via pH-dependent and –independent mechanisms. Neurosci. Res. **38**:265-271.

19. **Morihata, H., F. Nakamura, T. Tsutada, and M. Kuno.** 2000. Potentiation of a voltage-gated proton current in acidosis-induced swelling of rat microglia. J. Neurosci. **20**:7220-7227.
20. **Nanda, A. and S. Grinstein.** 1991. Protein kinase C activates an H^+ (equivalent) conductance in the plasma membrane of human neutrophils. Proc. Natl. Acad. Sci. USA. **88**:10816-10820.
21. **Niida S., M. Kaku, H. Amano, H. Yoshida, H. Kataoka, S. Nishikawa, K. Tanne, N. Maeda, S. Nishikawa, and H. Kodama.** 1999. Vascular endothelial growth factor can substitute for macrophage colony-stimulating factor in the support of osteoclastic bone resorption. J. Exp. Med. **190**:293-298.
22. **Nordström, T., O. D. Rotstein, R. Romanek, S. Asotra, J. N. Heersche, M. F. Manolson, G. F. Brisseau, and S. Grinstein.** 1995. Regulation of cytoplasmic pH in osteoclasts. Contribution of proton pumps and a proton-selective conductance. J. Biol. Chem. **270**:2203-2212.
23. **Nordström, T., L. D. Shrode, O. D. Rotstein, R. Romanek, T. Goto, J. N. Heersche, M. F. Manolson, G. F. Brisseau, and S. Grinstein.** 1997. Chronic extracellular acidosis induces plasmalemmal vacuolar type H^+ ATPase activity in osteoclasts. J. Biol. Chem. **272**:6354-6360.
24. **Rousselle, A. –V. and D. Heymann.** 2002. Osteoclastic acidification pathways during bone resorption. Bone **30**:533-540.
25. **Sakai, H., F. Nakamura, and M. Kuno.** 1999. Synergetic activation of outwardly rectifying Cl^- currents by hypotonic stress and external Ca^{2+} in murine osteoclasts. J. Physiol. **515**:157-168.
26. **Sakuta, K., H. Morihata, H. Mori, H. Sakai, and M. Kuno.** 2002. Cell swelling as an intermediate signal leading to activation of a Cl^- channel in extracellular calcium-sensing of murine osteoclasts. Osaka City Med. J. **48**:29-38.
27. **Sakuta, K., H. Sakai, H. Mori, H. Morihata, and M. Kuno.** Na^+-dependence of extracellular calcium-sensing mechanisms leading to activation of an outwardly rectifying Cl^- channel in murine osteoclasts. Bone. **31**:374-380.
28. **Shibata, T., H. Sakai, and F. Nakamura.** 1996. Membrane currents of murine osteoclasts generated from bone marrow/stromal cell co-culture. Osaka City Med. J. **42**:93-107.
29. **Shibata, T., H. Sakai, F. Nakamura, A. Shioi, and M. Kuno.** 1997. Differential effect of high extracellular Ca^{2+} on K^+ and Cl^- conductances in murine osteoclasts. J. Memb. Biol. **158**:59-67.
30. **Steinbeck, M. J., W. H. Appel, Jr., A. J. Verhoeven, and M. J. Karnovsky.** 1994. NADPH-oxidase expression and in situ production of superoxide by osteoclasts actively resorbing bone. J. Cell Biol. **126**:765-772.
31. **Suzuki K., B. Zhu, S. R. Rittling, D. T. Denhardt, H. A. Goldberg, C. A. McCulloch, and J. Sodek.** 2002. Colocalization of intracellular osteopontin with CD44 is associated with migration, cell fusion, and resorption in osteoclasts. J. Bone Miner. Res. **17**:1485-1497.
32. **Yang, S., P. madyastha, S. Bingel, W. Ries, and L. Key.** 2001. A New Superoxide-generating oxidase in murine osteoclasts. J. Biol. Chem. **276**:5452-5458.